

RSC Advances



This is an *Accepted Manuscript*, which has been through the Royal Society of Chemistry peer review process and has been accepted for publication.

Accepted Manuscripts are published online shortly after acceptance, before technical editing, formatting and proof reading. Using this free service, authors can make their results available to the community, in citable form, before we publish the edited article. This *Accepted Manuscript* will be replaced by the edited, formatted and paginated article as soon as this is available.

You can find more information about *Accepted Manuscripts* in the [Information for Authors](#).

Please note that technical editing may introduce minor changes to the text and/or graphics, which may alter content. The journal's standard [Terms & Conditions](#) and the [Ethical guidelines](#) still apply. In no event shall the Royal Society of Chemistry be held responsible for any errors or omissions in this *Accepted Manuscript* or any consequences arising from the use of any information it contains.

Ab-initio studies of electric field gradients and magnetic properties of uranium dipnictides

E. Ghasemikhah,¹ S. Jalali Asadabadi,^{1,} Iftikhar Ahmad,^{2,3**} and M. Yazdani-Kacoei¹*

¹Department of Physics, Faculty of Science, University of Isfahan (UI), Hezar Gerib Avenue, Isfahan 81746-73441, Iran

²Center for Computational Materials Science, University of Malakand, Chakdara, Pakistan

³Department of Physics, University of Malakand, Chakdara, Pakistan

* *Corresponding author:* *Saeid Jalali-Asadabadi, Ph.D. (IUT, Iran)*
Department of Physics, Faculty of Science,
University of Isfahan (UI), Hezar Gerib Avenue,
Isfahan 81746-73441, Iran
saeid.jalali.asadabadi@gmail.com, sjalali@sci.ui.ac.ir
 (+989133287908)

** *Corresponding author:* *Iftikhar Ahmad Ph.D. (Idaho, USA)*
Center for Computational Materials Science
University of Malakand, Chakdara, Pakistan
ahma5532@gmail.com (092)332-906-7866

ABSTRACT

In this paper, we explore the electric field gradients (EFGs) at ²³⁸U sites for antiferromagnetic UX₂ (X=P, As, Sb, Bi) using LDA, LDA+U, GGA, GGA+U, and exact exchange for correlated electrons schemes by considering the diagonalization of the spin-orbit coupling Hamiltonian in the space of the scalar relativistic eigenstates using the second-order variational procedure. The electronic structures and magnetic properties of the compounds are also investigated. It is found that the density functional theory approaches except exact exchange for correlated electrons are not successful in reproducing the experimental zero electric field gradient value in UBi₂, even LDA+U and GGA+U within their default 4f density matrices by varying the U parameter in an energy interval of [0; 4 eV], though these techniques with no need to manually adopt their initial conditions (elements of the occupation matrix) are effective in the calculation of the nonzero electric field gradients for the other compounds. The exact exchange for correlated electrons has efficiently provided the null electric field gradient in UBi₂ and nonzero electric field gradients for the other compounds by adjusting its dimensionless parameter α to 0.4. The physics of the null electric field gradient in UBi₂ is revealed in this article and it is discussed that the source of the ignorable electric field gradient originates from the antiferromagnetic ordering of $\uparrow\downarrow$ as compared to the long-range antiferromagnetic ordering of $\uparrow\uparrow\downarrow\downarrow$ in the other compounds. Furthermore, our calculated magnetic moments for the uranium atoms in these compounds are consistent with the available experimentally measured values as compared to the severely underestimated theoretical results.

Key Words: Uranium dipnictides; electric field gradients; strongly correlated electron systems; heavy fermions; ab-initio studies

I. INTRODUCTION

Electric field gradient (EFG) is a powerful tool to investigate atom in a crystalline environment.¹ It reveals the deflection of electron cloud around the nucleus from spherical mode, where larger value of this parameter means more asymmetry from the spherical shape. Therefore, in crystals EFG serves as a prevailing criterion for the measurement of the electron's localization within an atom.² The electric quadruple moment (Q) and EFG are nonzero for all nuclei with a nuclear quantum number equal or higher than one.³

The principle component of the electric field gradient (EFG) tensor, V_{zz} , is used to reveal the asymmetry of electrons around a nucleus. This value sensitively indicates the amount (orientation) of deviated electron charge density distributions (ECDDs) from spherical symmetry.⁴ The V_{zz} value is zero for spherical ECDDs and nonzero for asymmetrical ECDDs,⁵ where it serves as a very sensitive indicator to the asymmetry of semicore,⁶ valence states,⁷ and electron density of states (DOS).² Although V_{zz} is not a measurable quantity in the laboratory,¹ but it can be indirectly evaluated by a variety of accurate experimental techniques⁸, like Mössbauer spectroscopy, where in this technique the nuclear quadruple moment is measured and then the basic concept that the electric hyperfine splitting, ΔE_{hf} , is proportional to V_{zz} times nuclear electric quadruple moment (Q)¹ is used to evaluate V_{zz} . Interestingly this parameter connects ΔE_{hf} and Q, where one is a measurable condensed matter parameter and the other one a measurable nuclear quantity. Hence, V_{zz} may be generally considered as a connecting bridge between condensed matter physics and nuclear physics (indebted to the Mössbauer's discovery) and it can be precisely predicted by modern *ab-initio* density functional theory (DFT) calculations. In this work, we are interested in the theoretical condensed matter aspects of the V_{zz} for actinides specifically UX_2 (X=Bi, Sb, As, P) compounds.

The electronic and magnetic properties of actinide materials have always been a topic of interest in condensed matter physics because of their 5f electrons which display some remarkable physical properties such as, heavy fermions behavior, Pauli paramagnetism, spin fluctuation and unconventional superconductivity.⁹⁻¹⁵ The properties of a crystal depend on the localization of its electrons¹⁶, but the localization of the 5f electrons depends upon the crystal environment and hence the atomic radii for elements with 5f orbitals are not fixed¹⁵. The difference of the same actinide atom from one material to another mainly originates from the fact that the 5f electrons have a dual nature between itinerant and localized states.¹⁷ The 5f electrons have an intermediate property, something between the localization of the 4f electrons in the lanthanide compounds and the itinerant 3d electrons in the transition metals.¹⁸ Sometimes, the de Haas-van Alphen and Shubnikov-de Haas experiments are performed to clarify the nature of 5f electrons in a compound.^{18,19} Most of the actinides are extremely rare and therefore the main concentration of the experimental projects are focused on uranium compounds and uranium alloys.

The physical properties of uranium compounds are related to their lattice constants, the distance between U atoms and hybridization of 5f electrons with other valence electrons. According to the Hill criteria,²⁰ uranium based compounds with the U-U interatomic distances smaller than 3.4-3.6 Å are typically nonmagnetic with itinerant 5f states.²¹ Metallic uranium is paramagnetic but shows magnetic ordering when it combines with group 5 (N, P, As, Sb, Bi) or group 6 (S, Se, Te) elements. All UX_2 (X = Bi, Sb, As, P) actinide compounds are anti-ferromagnetic with relatively high Néel temperature. The magnetic ordering in these compounds is the consequence of the partially filled 5f shell.^{22,23} The anti-ferromagnetic structure of these compounds is determined by neutron diffraction, which shows that these compounds consist of ferromagnetic sheets of uranium stacked perpendicularly to the c axis.^{24,25} The magnetic ordering

for UBi_2 is $\uparrow\downarrow$, while for USb_2 , UAs_2 and UP_2 is $\uparrow\uparrow\downarrow\downarrow$. Therefore, the magnetic and chemical unit cells of UBi_2 are identical but in the other compounds the magnetic unit cell is double with respect to the chemical unit cell along the $[001]$ direction.^{17,26,27} The double magnetic unit cell in USb_2 , UAs_2 and UP_2 brings about a flat magnetic Brillouin zone.^{18,28,29}

The main focus of the present studies is to theoretically reproduce the experimental EFG values³⁰ at ^{238}U sites for antiferromagnetic UX_2 ($\text{X}=\text{P}, \text{As}, \text{Sb}, \text{Bi}$) dipnictides. These experiments which were performed at 5.1 K^{30} , reveal zero EFG value for UBi_2 and nonzero values for the other dipnictides. Therefore, along with the theoretical understanding of the EFGs for these compounds, the second main motivation of this study is to explore the cause of the zero EFG of the UBi_2 . The electronic structures and magnetic properties of the compounds are also investigated and discussed in details. The calculations are carried out with the different flavors of the density functional theory i.e., local density approximation (LDA), generalized gradient approximation (GGA), LDA plus Hubbard potential (LDA+U), GGA+U, and exact exchange for correlated electrons (EECE) to reveal the clear theoretical description of the compounds. As these compounds have 5f electrons which may have strong relativistic effects, so those expected relativistic effects are included by using the spin orbit coupling (SO) in our calculations.

II. COMPUTATIONAL DETAILS

The calculations presented in this paper have been performed within the framework of the density functional theory (DFT) using the augmented plane waves plus local orbitals (APW+lo) method as implemented in the WIEN2k code.³¹ In the APW+lo method the wave functions, charge density and potential are expanded in spherical harmonics within non-overlapping Muffin-tin spheres and in plane waves in the remaining interstitial region of the unit cell. The exchange correlation functional is treated with the LDA, GGA, LDA+U and GGA+U. It is worth

to mention that in these calculations we use LDA of Perdew-Wang 92 and GGA of Perdew-Bourke-Ernzerhof 96. The relativistic effects are included by diagonalizing the spin-orbit (SO) coupling Hamiltonian in the space of scalar relativistic eigenstates using the second-order variational procedure³² in our calculations for the proper treatment of the 5f electrons of uranium.

It is well understood that the most popular approximations for the exchange correlation functional in the DFT³³ are the local density approximation (LDA)³⁴⁻³⁶ and the generalized gradient approximation (GGA)³⁷⁻⁴⁰. These approximations in most regular cases give appropriate results, consistent with the experimental values. The main reason for using these local schemes is that they lead to calculations which are computationally cheap in comparison to the more sophisticated schemes. These functionals have some shortcomings, which have been revealed over time. The main shortcoming of these approximations is that they have problems to describe the electronic structure of strongly correlated compounds, whereas strongly correlated systems have attracted enormous attention in physics research in the recent years. The importance of the strongly correlated systems and the shortcoming of LDA or GGA approximation in describing these systems encourage researchers to think about new solution to this problem. The DFT approach with Hubbard parameter such as LDA+U and GGA+U is one of the solutions to the problems of the strongly correlated systems.⁴¹⁻⁴⁴ The number of calculations using this scheme, since the 1990 decade, has shown that this approach has a specific role in the electron correlation of crystals. Nevertheless, this approach has also some disadvantages, e.g., for applying this method, one needs to know the U_{eff} (U-J) parameter whereas its determination is time consuming theoretically and costly in experiments. Furthermore, perchance in some cases by using these functionals too we cannot obtain the acceptable results that are compatible with the experimental

results due to the fact that their predicted self-consistent results in some cases can depend on the initial conditions, i.e., the so called multiple solutions problem.⁴⁵ In orbital dependent schemes, the initial conditions, i.e., the elements of the occupation matrices can be manually adapted (by performing several self-consistent calculations for a variety of occupation matrices and eventually selecting the one which leads to the minimum energy) to achieve consistent results with experiment. But, this task can be also time consuming for the 4f-electron systems with angular momentum quantum number $l=3$ having two real and complex $(2l+1)\times(2l+1)=7\times 7$ density matrices. Although the hybrid method is also orbital dependent, fortunately for the cases under study can give excellent results by adjusting only its alpha parameter. We show that the exact exchange for correlated electrons (EECE) method can be considered as a successful approach to study our systems which was presented in 2006 by Novák et al.^{46,47} The EECE scheme in many cases leads to acceptable results for strongly correlated systems. Therefore, in order to achieve logical theoretical results we are also using EECE beside the other functionals mentioned earlier.

To avoid the overlap of the Muffin-tin spheres during the calculations; the Muffin-tin sphere of radius 2.8 a.u. is chosen for U in UBi_2 , USb_2 , UAs_2 but 2.6 a.u. in UP_2 and 2.4 a.u. is chosen for X in UX_2 compounds. The experimental lattice parameters measured by X-ray diffraction technique,^{24,48} shown in Table 1, are used as input parameters. For sampling of the Brillouin zone, a mesh of 45 special k-points which corresponds to the grids of $10\times 10\times 5$ is used for UBi_2 , while $11\times 11\times 2$ grids with 21 special k-points in the irreducible part of the Brillouin is used for the other compounds. The maximum ℓ for the waves inside the atomic spheres is confined to $\ell_{max} = 10$. The wave function in the interstitial region is expanded in plane waves with a cutoff of $R_{MT}K_{max} = 7$. The charge density is Fourier expanded up to $G_{max} = 14\sqrt{R_y}$.

The full relaxation is performed with the criterion of $1 R_y/Bohr$ on the exerted forces. In the LDA+U, GGA+U and EECE schemes, U and α parameters are gradually increased from about zero to values having converged calculations with enough accuracy.

TABLE 1. Lattice parameters (a and c) and lattice parameter ratio for UX₂ compounds.

Compound	a (Å)	c (Å)	c/a
UBi ₂	4.445	8.908	2.004
USb ₂	4.270	8.884	2.048
UAs ₂	3.954	8.116	2.053
UP ₂	3.810	7.764	2.038

III. RESULTS AND DISCUSSIONS

A. Electric Filed Gradients

The electric field gradient is a second order symmetric tensor with zero trace and five independent components. The experimental measurement and theoretical calculations of the electric field gradient is a tricky job. The EFG cannot be measured directly from experiments, therefore first one has to perform Mössbauer spectroscopy to measure nuclear quadruple interaction and then, calculate electric field gradient (EFG) by using relation $V_{zz} = \Delta E_{hf}/e^2Q$, where Q , e and ΔE_{hf} are nucleus quadruple moment, electron charge and electric hyperfine splitting, respectively.³⁰

As a matter of fact $f(I, m_I, \eta)$ is a well known function of the nuclear spin angular momentum quantum number I , and the magnetic quantum number m_I , as well as the axial

asymmetry parameter $\eta = \frac{V_{xx}-V_{yy}}{V_{zz}}$, where $V_{zz} \geq V_{yy} \geq V_{xx}$ in the principle axes system (PAS).⁴⁹

$Q(\eta)$ is zero for spherical nuclear charge distribution with $I = 0$ or $\frac{1}{2}$ (axially symmetric crystalline environments with $V_{xx} = V_{yy}$) and nonzero for nonspherical nuclear charge distribution with $I \geq 1$ (axially asymmetric crystalline environments with $V_{xx} \neq V_{yy}$).^{8,49} η vanishes due to the axially symmetric environments⁵ for the systems under question in this paper, viz. $f(I, m_I, \eta) = f(I, m_I)$, and can serve as a powerful gauge for measuring such a degree of localization.

After the above discussion it is obvious that the only parameter which can be determined at the uranium site in UX_2 (X=P, As, Sb, Bi) dipnictides is the principle component of EFG:^{3,50}

$$V_{zz} = \lim \left[\frac{5}{\pi} \right]^{1/2} \left[V_{20} / r^2 \right] \quad (1)$$

where, V_{20} is the radial potential and can be calculated as:³

$$V_{20}(r=0) = \frac{4\pi}{5} \int_0^{R_{MT}} \frac{\rho_{20}}{r} dr - \frac{4\pi}{5} \int_0^{R_{MT}} \frac{\rho_{20}}{r} \left(\frac{r}{R_{MT}} \right)^5 dr \quad (2)$$

$$+ 4\pi \sum_k V(\hat{k}) J_2(kR_{MT}) Y_{20}(\hat{k})$$

where, ρ_{20} is the $L = 2$ and $M = 0$ of density expansion, $Y_{20}(\hat{k})$ is spherical Bessel function and R_{MT} is the Muffin-tin (MT) sphere radius. The first term in Eq. (2) is related to valence electrons (Quasi-core) in MT sphere. It is called valence contribution of EFG and indicated with V_{zz}^{val} . The sum of the second and third term is related to out MT sphere electrons and interstitial region and therefore is known as lattice contribution of EFG and is indicated by V_{zz}^{lat} .³

The calculated EFGs and their valence and lattice parts for UX_2 (X=Bi, Sb, As, P) compounds using LDA, GGA, LDA+SO, GGA+SO, LDA+U and GGA+U, are presented in Table 2. The calculated values of the EFGs are also compared with the EFG values evaluated from the

Mössbauer spectroscopy³⁰. The table clearly indicates nonzero calculated EFG values for USb₂, UAs₂, and UP₂, through GGA, LDA+U and GGA+U approximations. Though, these results are underestimated from the experimental values but still provide a clue that the charge distribution is not symmetric. Unlike these deliberations, these approximations are not successful in attaining the zero EFG value for UBi₂. In the expectation of further elaboration, here, we have not tried to adjust the elements of occupation matrix to force the LDA+U or GGA+U to reproduce the experimental values. Instead, in order to reach zero value for the EFG of UBi₂, only the Hubbard parameter (U) in LDA+U and GGA+U approximations are varied from *0.01* to *0.40 Ry*. Fig. 1 shows the effect of U on the EFG value of UBi₂. It is clear from the figure that the EFG increases with U, consequently the difference of the calculated value increases from the experimental results and hence none of the used “U” value provides correct EFG for UBi₂. On the other hand for U higher than *0.40 Ry*, calculations are not well converged and antiferromagnetic property of UBi₂ vanishes. So, results of calculations for U higher than *0.40 Ry* are not presented here. The results presented in Table 2 and Fig. 1 confirms that these approximations are not suitable to calculate EFG for UBi₂ and we may use some appropriate methods and approximation for this compound. Although, these approximations are not bad choices for the other UX₂ compounds, as they provide results which are in somewhat manner comparable with the experimental values. The strong influence of U on the electronic properties of the UBi₂ confirms that this compound is strongly correlated electron system. So, to resolve the issue we need to be more careful in the choice of the exchange-correlation energy for the treatment of this compound. In order to resolve this issue we proceed with another exchange-correlation energy which is more suitable for the strongly correlated compounds, called exact exchange for correlated electrons (EECE) scheme,

introduced by Novák et al.⁴⁶ in 2006. The method of performing the EEC calculations is like LDA+U. Therefore, they are called U-like functionals. The calculated results by using these

TABLE 2. Summary of EFG V_{zz} in units $10^4 V nm^{-2}$, also the lattice (V_{zz}^{lat}) and valence (V_{zz}^{val}) contribution of EFGs from LDA, GGA, LDA+U and GGA+U calculations.

Compound		LDA	GGA	LDA+SO	GGA+SO	LDA+U	GGA+U	EXP. ^a
UBi ₂	V_{zz}^{tot}	0.523	0.556	0.545	0.558	0.532	0.645	0±0.2
	V_{zz}^{val}	0.524	0.560	0.543	0.558	0.528	0.641	-
	V_{zz}^{lat}	-0.001	-0.004	0.002	0.000	0.004	0.004	-
USb ₂	V_{zz}^{tot}	1.237	1.227	1.287	1.275	1.182	1.195	1.6±0.4
	V_{zz}^{val}	1.242	0.241	1.289	1.286	1.179	1.190	-
	V_{zz}^{lat}	-0.005	-0.014	-0.002	-0.011	0.003	0.005	-
UAs ₂	V_{zz}^{tot}	1.409	1.353	1.412	1.365	1.306	1.303	1.5±0.3
	V_{zz}^{val}	1.414	1.357	1.417	1.368	1.305	1.303	-
	V_{zz}^{lat}	-0.005	-0.004	-0.005	-0.003	0.001	0.000	-
UP ₂	V_{zz}^{tot}	1.544	1.423	1.501	1.391	1.260	1.244	2.1±0.5
	V_{zz}^{lat}	1.549	1.428	1.505	1.395	1.260	1.244	-
	V_{zz}^{val}	-0.005	-0.005	-0.004	-0.004	0.000	0.000	-

^aReference 30.

functionals are presented in Table 3. It is clear from the table that all these functionals lead to acceptable values of EFGs for UBi_2 , which are in agreement with the experimental results. A general form of the EECE functional can be written as follows⁴⁶:

$$E[\rho, \{\phi_m\}] = E^{SL}[\rho] + E_x^{HF}[n^{\sigma\sigma'}(\rho), \{\phi_m\}] - E_{dc}[n^{\sigma\sigma'}(\rho), \{\phi_m\}], \quad (3)$$

where, ϕ_m represents the correlated orbitals, E^{SL} is the energy of the semilocal functional such as LDA or GGA, E_x^{HF} is the exchange energy which is calculated using the Hartree-Fock approach, and the last term is the double counting correction which can be written as:

$$E_{dc}[n^{\sigma\sigma'}(\rho), \{\phi_m\}] = E_{xc}^{SL}[\rho_{corr}]. \quad (4)$$

According to these equations, the EECE approach improves the exchange-correlation energy of semilocal functionals using the exact exchange energy of Hartree-Fock method and as a result improves the semilocal functional results with respect to the experiments. This originates from the localized character of U-5f electrons which is well described by the EECE approach.

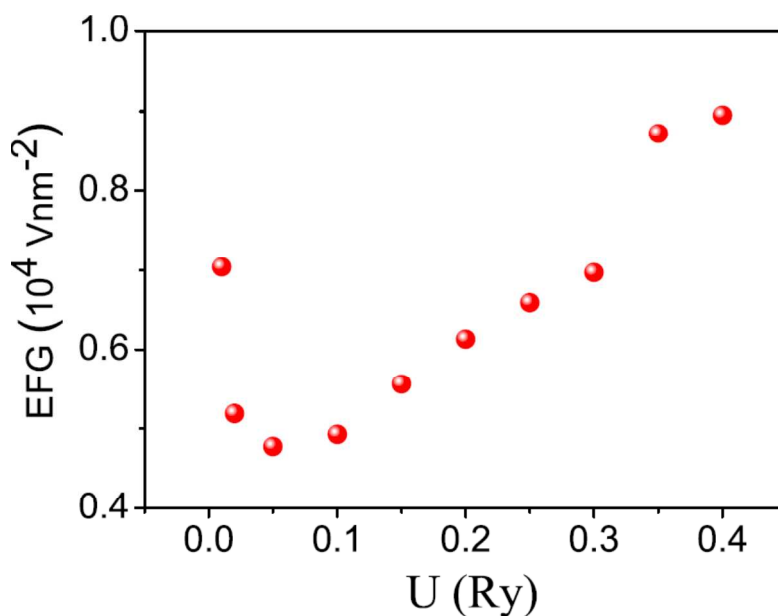


FIG. 1. (Color online) The electric field gradients using different Hubbard parameters in LDA+U

TABLE 3. Summary of EFG V_{zz} in units $10^4 V nm^{-2}$, also the lattice (V_{zz}^{lat}) and valence (V_{zz}^{val}) contribution of EFGs from EECF calculations.

Compd		LDAFock	B3PW91	WCFock	PBEsol	PBEFock	EXP. ^a
UBi ₂							
	V_{zz}^{tot}	0.108	0.118	0.065	0.050	-0.057	0±0.2
	V_{zz}^{val}	0.103	0.099	0.062	0.056	-0.066	-
	V_{zz}^{lat}	0.005	0.019	0.003	-0.006	0.009	-
USb ₂							
	V_{zz}^{tot}	1.277	1.293	1.261	1.280	1.283	1.6±0.4
	V_{zz}^{val}	1.275	1.289	1.258	1.278	1.280	-
	V_{zz}^{lat}	0.002	0.004	0.003	0.002	0.003	-
UAs ₂							
	V_{zz}^{tot}	1.346	1.377	1.311	1.317	1.295	1.5±0.3
	V_{zz}^{val}	1.346	1.378	1.311	1.317	1.295	-
	V_{zz}^{lat}	0.000	-0.001	0.000	0.000	0.000	-
UP ₂							
	V_{zz}^{tot}	1.269	1.202	1.246	1.262	1.215	2.1±0.5
	V_{zz}^{lat}	1.269	1.201	1.245	1.261	1.215	-
	V_{zz}^{val}	0.000	0.001	0.001	0.001	0.000	-

^aReference 30.

The EECF functionals reproduce the experimental zero EFG of UBi₂, which was at least time consuming if not impossible for the other DFT schemes. The calculated EFG for the other UX₂ compounds are also close to the experimental values, except the results for UP₂, which has

larger difference than the experimental results as compared to those of the LDA and GGA. In fact, in UP_2 case, the approximations with Hubbard parameters such as LDA+U and GGA+U are also not successful to calculate EFG, and so does is EECE which is a U-like method. The lattice and valence parts of EFG for UX_2 compounds are also shown in Table 2 and Table 3. One can see from these values that almost all of EFG is related to the valence electrons in the MT sphere and the electrons which are out of MT sphere do not significantly affect EFG. Therefore, in the EFG calculations, it is essential to choose appropriate MT sphere radii otherwise one can obtain wrong EFG value. On the other hand lattice parameters do not substantially affect EFG, since out of MT sphere electrons have no significant effect on it, and therefore we can use experimental lattice parameters in the EFG calculations.

It is clear from Fig. 2-(a) that the EECE functionals provide good results in case of UBi_2 for $\alpha=0.40$. The calculations do not converge for α larger than 0.40 , and in case if the self-consistent calculations are elaborated to be converged, then the antiferromagnetic character of the crystal would be destroyed, because in this case the up and down density of states curves of the crystal are not symmetric and thereby cannot cancel each other to form zero antiferromagnetic feature. Keeping all these aspects in considerations, the EFG values presented in Table 3 of UBi_2 are calculated for $\alpha=0.40$. The same problems are observed during the EFG calculations of USb_2 , UAs_2 and UP_2 , but in these compounds the appropriate value for α is optimized to be 0.20 . Therefore, this value is used in the EECE functionals results of USb_2 , UAs_2 and UP_2 , shown in Table 3. It is clear from the table that these values are closer to the experimental values. If the convergence and antiferromagnetism problems for α higher than 0.20 were not there, then we could have reproduced the experimental EFG values for these compounds.

The interesting point that needs to be addressed here is the reason for the difference between EFG of UBi_2 and that of the other compounds. It is necessary to find the physics behind the question, why nuclear quadrupole interaction and EFG is zero for UBi_2 and non-zero for the other compounds? To answer these questions, the first logical step is to know factors that affect EFG value. Hence, we obtained p-p, d-d and f-f orbital contributions of EFG for UBi_2 and UAs_2 . Uranium atoms in the unit cell of UBi_2 are in the same position as UAs_2 ; but with special magnetic structure its ferromagnetic sheets order antiferromagnetically $\uparrow\downarrow$. In other words the

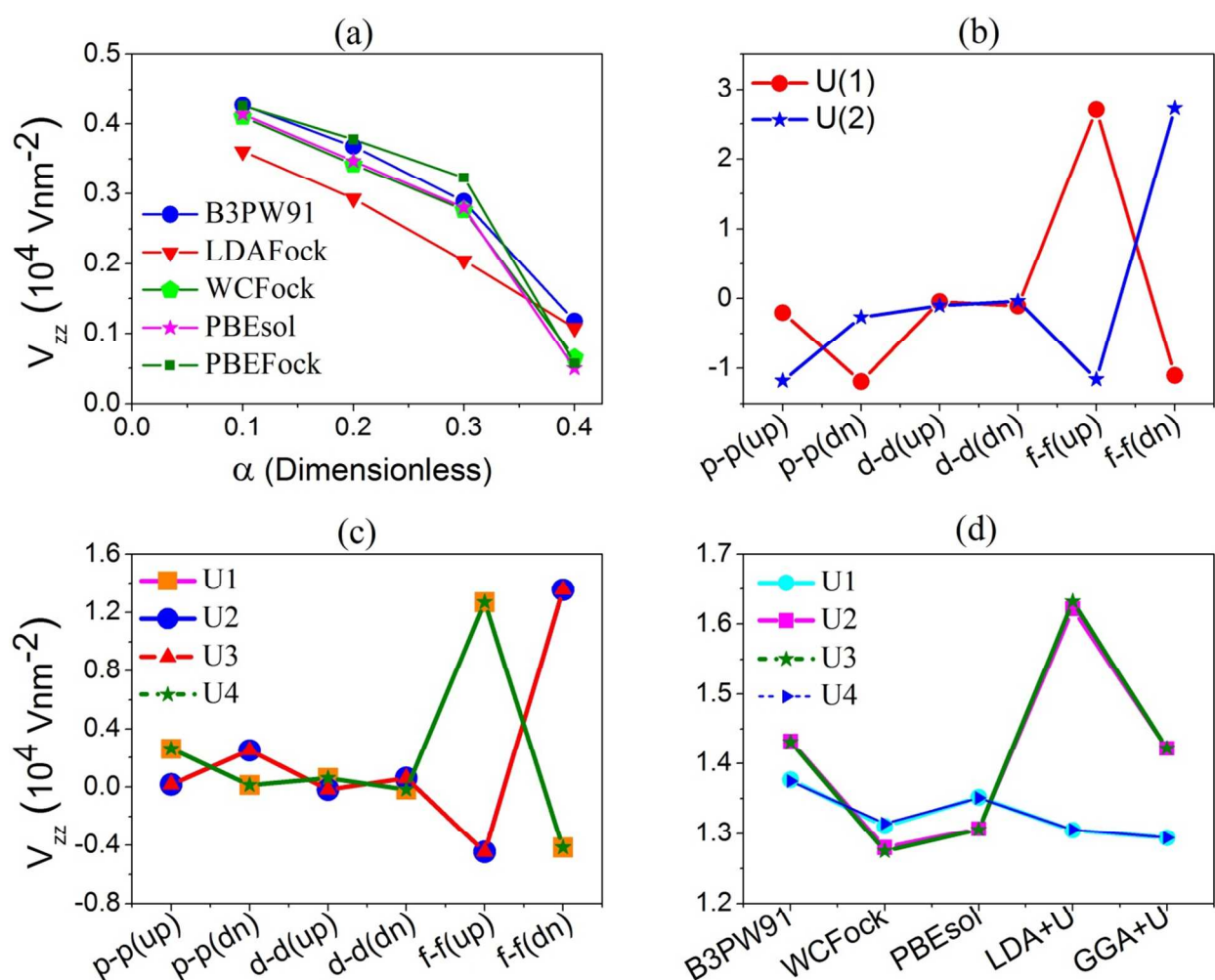


FIG. 2. (Color online) (a) V_{zz} values using different α in ECE functionals. Orbital contributions in V_{zz} for all uranium atoms using LDAFock approximation in (b) UBi_2 and (c) UAs_2 compounds. (d) V_{zz} 's for all uranium atoms in UAs_2 compound.

distribution of the magnetic or spin of atoms in a unit cell is different for UBi_2 than UAs_2 , though both have the same crystal structure. Fig.2-(b) shows orbital contributions of U(1) and U(2) atoms in the EFG of UBi_2 . It is clear that different contributions with up and down spin states are different for each atom. Also, different up and down contributions of both uranium atoms are reversely very close; that is, p-p orbital contribution of U(1) with up spin is close to that of U(2) with down spin.

The magnetic structure of UAs_2 is shown in Fig.3-(c), where it is obvious that for this compound U(1) and U(3) are at the same position but have opposite spins and similarly U(2) and U(4) are at the same positions but magnetically opposite to each other. However, U(1) and U(4) atoms, as well as, U(2) and U(3) atoms are magnetically the same, though their positions are different. Fig.2-(c) shows the p-p, d-d and f-f contributions of EFG for up and down spin states for all uranium of UAs_2 compound. This figure demonstrates that the magnetic structure for U(1) is similar to U(4) and for U(2) is similar to U(3), whereas the U(2) is arranged antiferromagnetically with the U(3) in EFG. The total EFG at all uranium atoms sites of UAs_2 for different approximations is shown in Fig.3-(d). This figure shows that for all approximations, the total EFG of U(1) and U(4) together, and total EFG of U(2) and U(3) are consistent. After the analysis of the EFG of UBi_2 and UAs_2 we can infer that the magnetic structure and spin arrangement of atoms have a significant effect on the EFG in uranium atoms position. Therefore, orbitals which have more magnetic properties have greater effect on EFG. Therefore, it seems that the main reason of the difference between the EFG of UBi_2 and the other UX_2 compounds is their difference in magnetic structures, because their spatial structure and point group are the same.

To examine this idea, we considered magnetic structure I for USb_2 , UAs_2 , UP_2 , as shown in Fig. 3(b), and magnetic structure II for UBi_2 , as shown in Fig. 3(c), and then calculate EFG at uranium site in these new structures. The calculated results presented in Table 4 show that the EFG of UBi_2 using structure II is $1.24 \times 10^4 \text{ Vnm}^{-2}$, while for structure I it is $0.11 \times 10^4 \text{ Vnm}^{-2}$, whereas the EFG of USb_2 is $0.09 \times 10^4 \text{ Vnm}^{-2}$ for structure I, and $1.28 \times 10^4 \text{ Vnm}^{-2}$ for structure

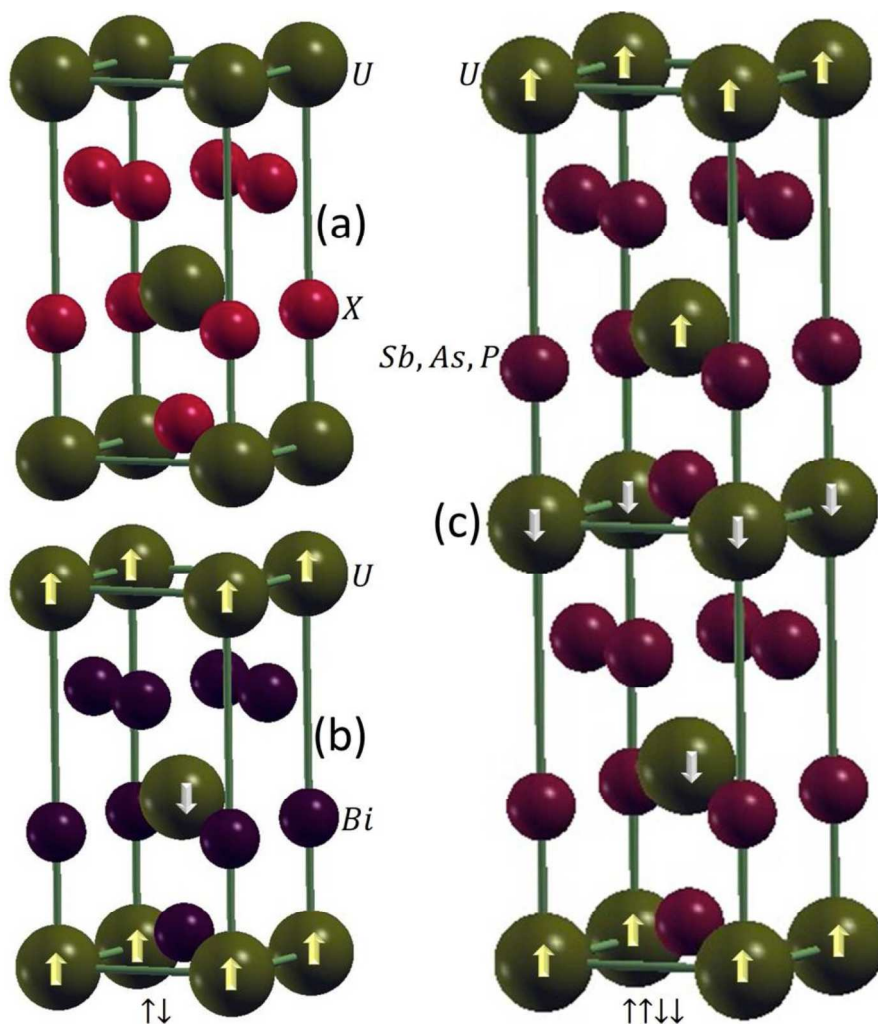


FIG. 3. (Color online) (a) Chemical structure for UX_2 ($X=Bi, Sb, As, P$), (b) magnetic structure of UBi_2 called as (I) and magnetic structure of USb_2 , UAs_2 and UP_2 compounds called as (II).

II. The quantity for UP_2 using structure I is as small as $0.12 \times 10^4 \text{ Vnm}^{-2}$ and very large for structure II. The EFG of UBi_2 with structure I is consistent with that of the USb_2 . Regarding to EFG of UX_2 compounds with different magnetic structures and previous discussion about the relationship between EFG and spin of atoms, it is concluded that the different EFG value of UBi_2 originates from the difference in the magnetic structure.

TABLE 4: The EFGs values for UX_2 compound in 10^4 V nm^{-2} units at different structures.

	UBi_2	USb_2	UAs_2	UP_2
Structure I	0.11	0.09	-	0.12
Structure II	1.24	1.28	1.35	1.27

The EFG of an atom can be different in different compounds containing this atom, as there are many factors affecting the EFG value. This means that for a specific atom we can have zero EFG in one compound and non-zero for another one. This is due to the fact that the point symmetry and magnetic structure of a cell affect EFG. Furthermore, external factors are also affecting EFG, whereas one of those factors is temperature. There are two equations for EFG at zero and 'T' temperature, regarding the partially filled orbitals and type of electrons. For s, p and d orbitals it is given below:⁵¹

$$V_{zz}(T) = V_{zz}(0)(1 - BT^{1.5}) \quad (5)$$

This is a nonlinear relation. For f orbitals we have:⁵¹

$$V_{zz}(T) = V_{zz}(0)(1 - BT) \quad (6)$$

where $V_{zz}(0)$, $V_{zz}(T)$, B and T are EFG at zero temperature, EFG at T temperature, a constant (which is in the order of 10^{-5} to 10^{-4}) and temperature, respectively. These equations show that

EFG decreases as temperature increases. We used density functional calculations which are performed at zero temperature, but experimental results are obtained at room temperature; therefore Eq. (6) is used to obtain EFG at room temperature. In order to consider temperature effect in EFG, we supposed that B is 10^{-4} . The EFG values of all UX_2 compounds at zero and 300K are shown in Table 5. The results clearly indicate that the EFG decreases as temperature increases but this decrease is not profound for 300K, though these results at zero temperature are reasonable as they can be confidently compared to the experimental data. It is obvious that with the increase in temperature electrons are excited and matter is expanded. It is also known that the EFG represents the asymmetry of electrons around a nucleus, therefore with the increases in temperature the asymmetry in electron decreases which consequently decrease the EFG.

TABLE 5: The EFGs values for UX_2 compound in 10^4 V nm^{-2} unit at different temperatures.

	UBi ₂	USb ₂	UAs ₂	UP ₂
T = 0 K	0.050	1.280	1.317	1.262
T = 300 K	0.049	1.242	1.277	1.224

B. DENSITY OF STATES

The density of states (DOS) curve shows the distribution of electronic state in terms of energy. The area under DOS curve in each energy interval is equal to the number of allowed electronic states in that interval. Fig.4 shows total, U and X atoms DOSs for all UX_2 compounds. In this figure, plots (a) to (d) show the total DOS curves for UX_2 compounds. All curves coincide with the Fermi level at non-zero value, so these compounds are conductors. The symmetry in the up

and down states for all the compounds shows that they are antiferromagnetic materials in nature. A valley in the DOS of USb_2 , UAs_2 and UP_2 can be seen in the energy interval 0 to 0.5eV but this valley goes far away from the Fermi level for UBi_2 and occurs around -1eV. The DOS of UBi_2 at the Fermi level and around it and especially far below the Fermi level states are more split and have less degeneracy. Furthermore, the DOS of UBi_2 coincides with the Fermi level at smaller values than that of the other compounds, and the height of peaks in this energy interval is less than that of the others. Therefore, the contribution of the Fermi level electrons of UBi_2 in conduction is easier. It is further noted that at low energies -6.0 to -4.5 eV the tail of curve of UBi_2 reaches to zero sooner, and therefore the band width of UBi_2 is lesser than the other compounds.

The plots (e) to (h) of the figure show DOS curves for U(1) and U(2) atoms of UX_2 compounds. As seen, in all compounds, DOS for each uranium atom for up and down spin states are asymmetric. It demonstrates that uranium atoms are magnetic in all compounds and have a local magnetic moment. The DOS of the second uranium atom with a reverse spin arrangement as compared to the first atom is shown in these plots. The DOS of this atom in up and down spin states is reversely the same as the DOS of the first atom. That is, up states curves for U(1) is the same as the down spin state curve for U(2) and vice versa. Therefore, the magnetic moment which is caused by U(2) is equal but in opposite direction to that of U(1) and hence the net magnetic moment of the compound is zero. This means that the magnetic moment of U(2) atom is canceled by that of U(1) atom and as result no net magnetic moment is observed in the unit cell. As a result, although uranium atoms are magnetic, but they have no contribution in the total magnetic moment of these crystals. As discussed earlier about the magnetic structure that in all UX_2 compounds the number of uranium atoms in opposite spin directions is equal.

The DOS curves for X atoms of the UX_2 compounds are shown in Figs. 4-(i) to 4-(l). As shown, in all compounds the up and down states curves for X atoms are symmetric, which reveal that X atoms are non-magnetic. So, in all these compounds the magnetic sheets of uranium are separated with non-magnetic sheets of X atoms. It causes a quasi-two dimensional property of them. The comparison of the DOS of U and X atoms in Fig. 4 shows that for all UX_2 compounds the main contribution of DOS at the Fermi level is related to U atoms, whereas X atoms have dominant contribution at higher energies. Since both, DOSs of U and X atoms coincide the Fermi level at non-zero value, it reveals that all electrons of these compounds contribute in the

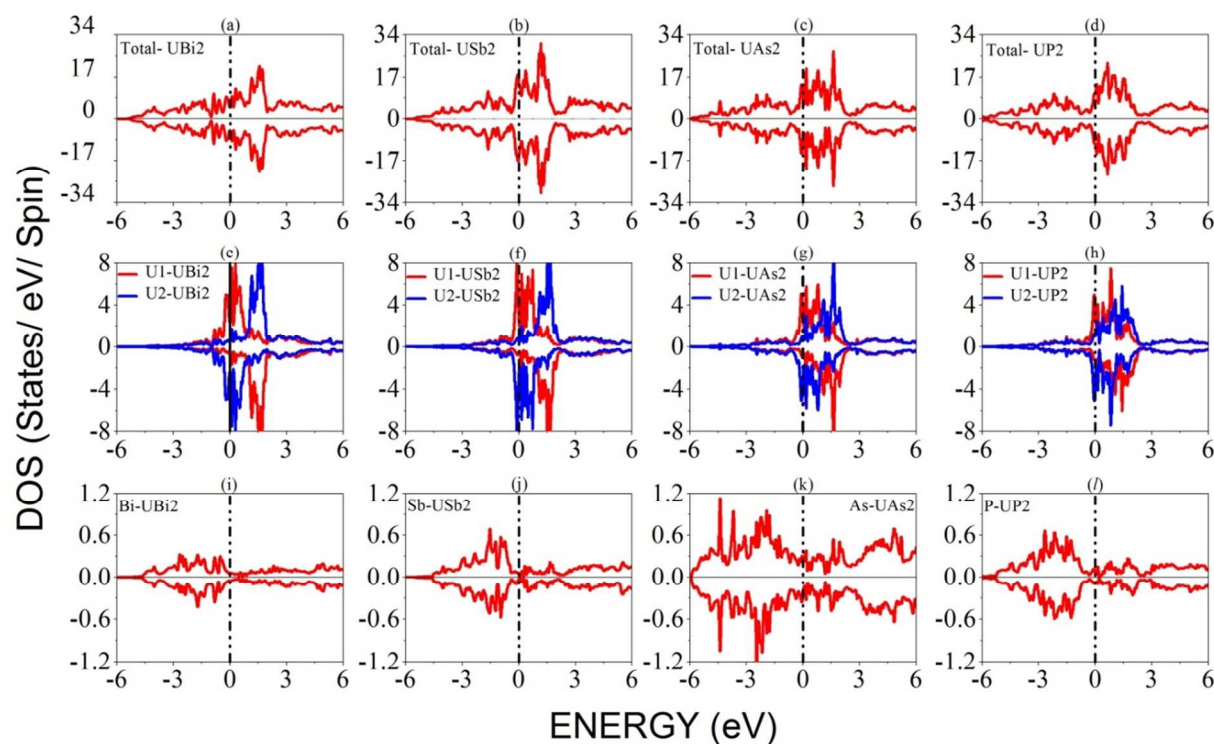


FIG. 4. (Color online) The DOS curves for: (a)-(d) The total UX_2 compounds, (e)-(h) The U(1) and U(2) atoms in all UX_2 compounds, (i)-(l) The X atoms in all UX_2 compounds.

conduction process. The comparison of the DOS of U and X atoms in Fig. 4 shows that for all UX_2 compounds the main contribution of DOS at the Fermi level is related to U atoms, whereas X atoms have dominant contribution at higher energies.

Fig. 5 shows the DOS curve for uranium orbitals in UBi_2 . All curves have non-zero value at the Fermi level, so all orbitals in uranium atom contribute in conduction. The DOS curve for f and d orbitals coincide the Fermi level at much higher energy than s and p orbitals, which shows that the electrons of these orbitals (f and d) are magnetic electrons of U and have more effect on the magnetic properties of the uranium atom. The DOS curves for uranium atom orbitals of the other UX_2 compounds are almost similar to Fig. 5, and therefore we have not shown them to avoid repetition.

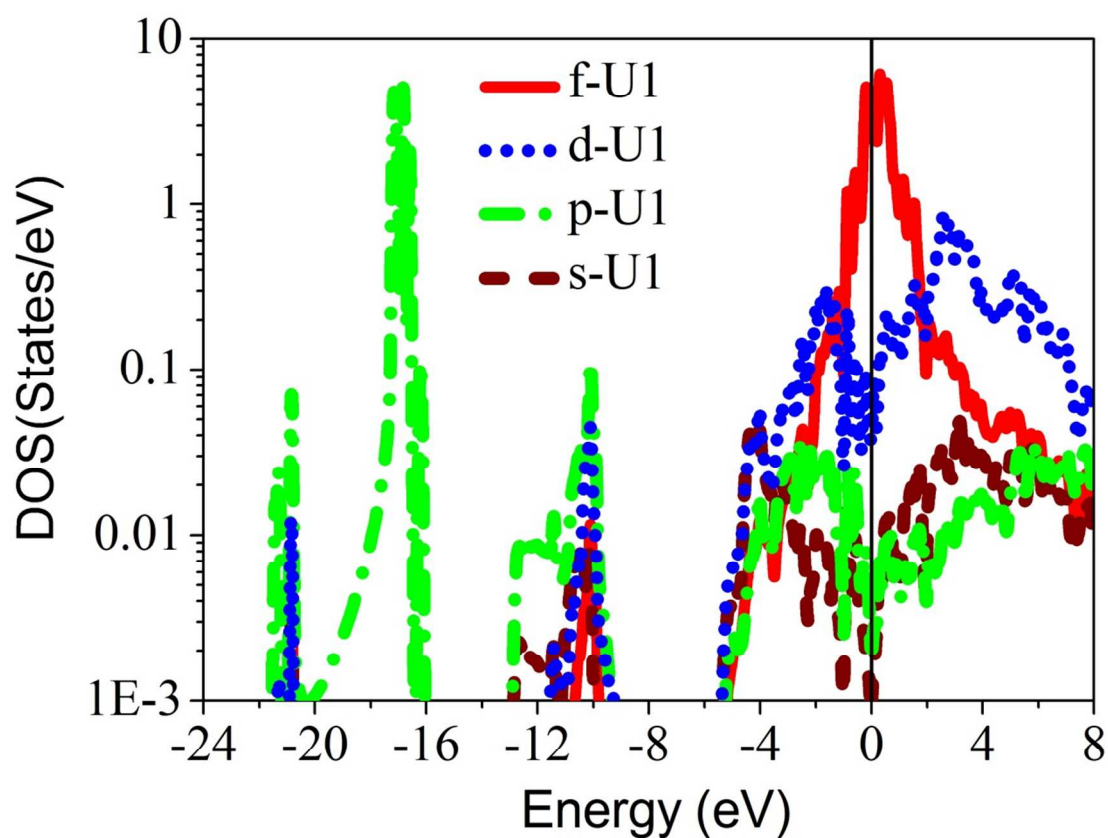


FIG. 5. (Color online) PDOS curves for all orbitals of uranium in UBi_2 compound.

The DOS curves for f and d orbitals of uranium are shown in Fig. 6, where the plots from (a) to (d) in this figure are related to the f orbital of uranium and (e) to (h) show d orbital. In all of the four compounds under study, the DOS of the up and down states are asymmetric, which shows magnetism for the electrons of this orbital. It is clear from the figure that the f orbital touches the Fermi level at non-zero value for all compounds, which confirms that the electrons of this orbital contributes in the conduction process. The high effective mass^{24,28} of the conduction carriers of these compounds is due to these electrons, though f is an internal orbital. These f orbital electrons are not completely localized, where the amount of localization is different for different compounds. Therefore, to investigate the localization of these orbitals we need case by case study of all the compounds. In all the compounds under study, the spin down electrons of the f orbital are easily participating in the conduction process as these electrons coincide the Fermi level at lower values, however the spin up electrons have a larger value at the Fermi level which shows higher effective mass of conduction carriers than that of the spin down electrons. The shape of DOS for f orbitals is the same as that of U atom.

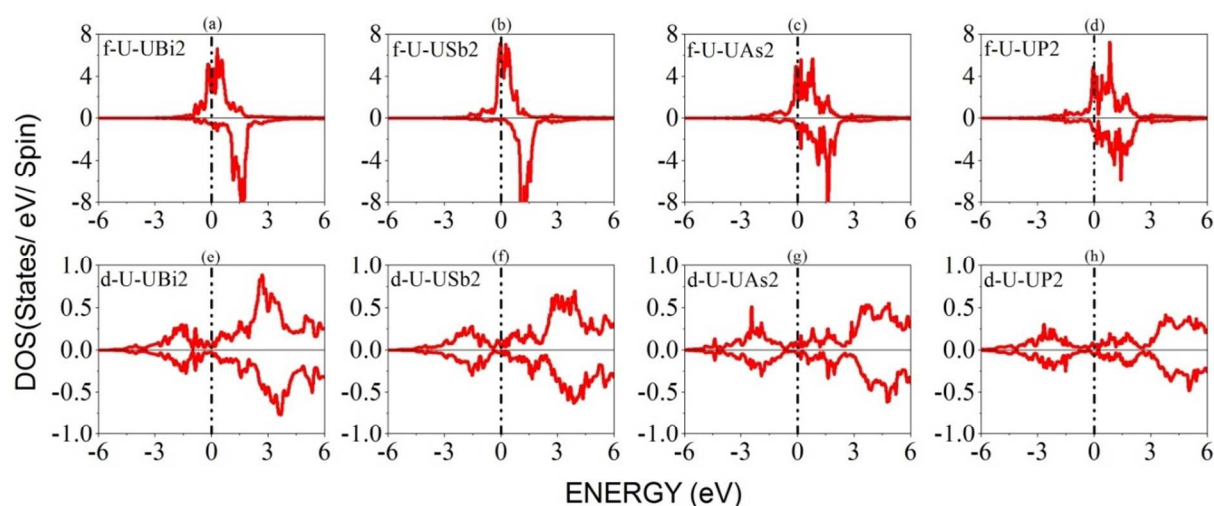


FIG. 6. (Color online) The PDOS curves of uranium atoms in UX_2 compounds. (a)-(d) The f orbitals and (e)-(h) The d orbitals.

The DOS of the d orbitals of uranium for up and down states for all the compounds shown in the figure display that these orbitals are symmetric for all compounds, and from area under the DOS curves we can say that the magnetic properties of f orbital is more than that of the d orbital, or in other words d is non-magnetic. As a result, the magnetic properties of uranium and consequently UX_2 compounds are due to the f orbital electrons. Therefore, the study of the f orbital electrons is important because they are strongly affecting the magnetic properties as well as high effective mass of conduction carriers of UX_2 compounds.

The partial DOS (PDOS) of f orbital of uranium in UBi_2 and USb_2 for various ℓ , m and $j(\ell \pm s)$ are shown in Fig. 7. There are 7 values for m in f orbital with $\ell = 3$. The plots in the figure from (a) to (c) show partial curves for $m = -3$ to $m = -1$. These plots show that the curves for UBi_2 and USb_2 are almost the same and their difference is only in the height of peaks, where for some energies the height of UBi_2 curve is higher while for other energies the height of USb_2 curve is a higher. The contribution of down spin states for energies lower than Fermi energy, i.e. occupied states, is very low and ignorable, where almost all of DOS curve in this energy interval is related to up spin states.

The PDOS of f orbital for $m = 1, 2$ and 3 are shown in the plots (d) to (f) of Fig. 7. The plots show that the contribution of these partial parts in occupied states is very low and most part of these curves are in the higher energies than the Fermi level and unoccupied states. It is also shown that the curves are shifted to the left towards the Fermi energy when m is decreased from 3 to 1. The curve for $m = 1$ exists at lower energy than the Fermi energy, but even in these parts, the contribution of the down states electrons in DOS of occupied states is very small. The plot (g) of the figure shows PDOS of f orbital for $\ell = 3$ and $m = 0$. This curve is also shifted to the left and has more contribution in occupied states relative to that of $m = 1, 2$ and 3 . Furthermore,

for $m = 0$ the contribution of the down spin states at lower than the Fermi energies is more than the other partial parts of the f orbital. However, this contribution is still lesser than the up spin states. In general, comparing the partial curves of f orbitals (figures 7-(a) to 7-(g)) we can see that most part of DOS of f orbital at lower than Fermi energies is related to negative and zero m . As the curves are expanded to the Fermi level with the change of m from $m = 3$ to $m = 1$, then the band width also increases in this region. Regarding the asymmetry of the up and down states of the partial parts, we can say that all parts with various m contribute in the magnetism of the

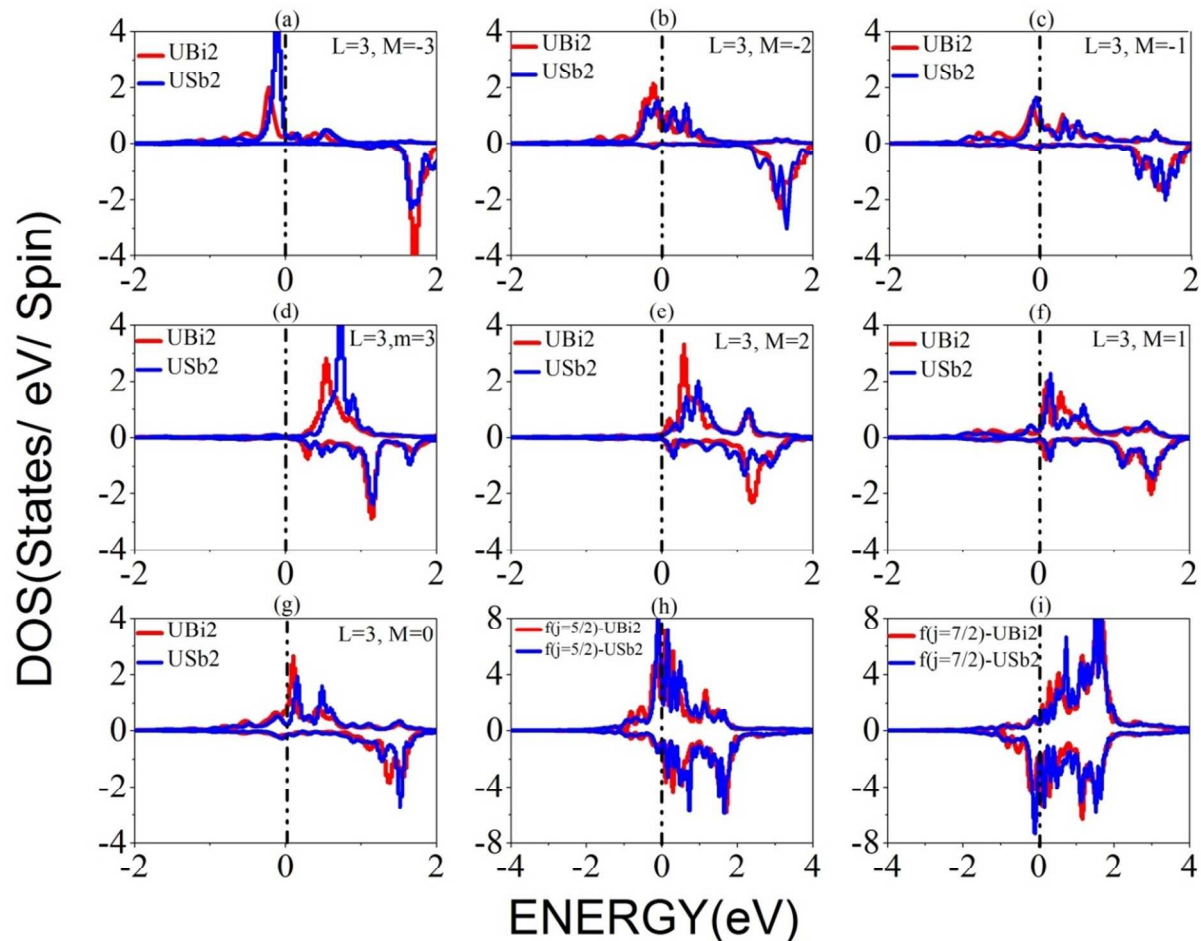


FIG. 7. (Color online) The PDOS curves of f orbital of uranium in UBi_2 and USb_2 compounds for various ℓ , m and j .

orbital. Fig.7 reveals that the up and down PDOSs are asymmetric with respect to each other for all m values. Thus, the PDOSs with different m values contribute in magnetism of f orbital. The curves for $m = 1, 2$ and 3 coincide the Fermi level at higher values, so the effective mass of conduction carriers is higher in these partial parts. Plots (h) and (i) of the figure show the partial curves of f orbitals of UBi_2 and USb_2 for $j = 5/2$ and $7/2$, respectively. It is clear from the plots that the behavior of DOS of these partial parts is almost the same for both crystals. For $j = 5/2$, the spin up states coincide Fermi level at higher value but in contrast for $j = 7/2$ the spin down states coincide the Fermi level at higher value. Therefore, the spin up states in $j = 5/2$ and spin down states in $j = 7/2$ have higher effective mass of conduction carriers. This reveals, easier conduction of f orbital electrons in the spin down states for $j = 5/2$ and spin up states for $j = 7/2$.

The detailed discussion on the magnetic properties of UX_2 ($X=\text{P, As, Sb, Bi}$) dipnictides reveals that these compounds are antiferromagnetic with short-range ordering of $\uparrow\downarrow$ for UBi_2 and long-range ordering of $\uparrow\uparrow\downarrow\downarrow$ for UP_2 , UAs_2 and USb_2 compounds. We also know from this study that the magnetic properties of these compounds are mostly originated from the uranium atoms especially from its f orbitals, whereas the d orbitals of uranium and X atoms are nonmagnetic. After all these considerations, it will not be appropriate if the magnetic moment of the uranium atom in these compounds is not discussed. Therefore, the magnetic moment of uranium atom in these compounds is calculated with WCFock approach and the calculated results are presented in Table 6. The calculated results are also compared with the experimental and other theoretical results. The comparison of the data presented in the table clearly indicates that the theoretical values of the magnetic moment of uranium atom in these compounds by Lebegue et al.¹⁷ are severely underestimated from the experimental results²⁴, however our calculated values for all

the compounds except UP_2 are consistent with the experimental results. The table also presents the contribution of the spin and orbital in the total magnetic moment of uranium for each compound. These results reveal that the orbital motion of the f-electrons has a profound effect on the magnetic properties of uranium atoms.

TABLE 6. Orbital (ORB), spin (SPI) and total (TOT) magnetic moments per uranium atom in μ_B using WCFock together with theoretical and experimental results of the others.

	UBi ₂	USb ₂	UAs ₂	UP ₂
ORB	-4.243	-3.904	-2.790	-2.221
SPI	1.887	1.681	1.209	0.947
TOT	2.365	2.223	1.645	1.274
TOT ^a	1.1±0.1	0.90±0.01	0.7±0.1	
EXP ^b	2.1±0.1	1.88±0.03	1.61±0.11	2.1±0.1

^aReference 17.

^bReference 24.

IV. CONCLUSIONS

In this paper, the electric field gradients (EFGs) and their lattice and valence contributions are calculated for UX_2 (X=Bi, Sb, As, P) compounds. The calculated results show that the EFG is zero for UBi₂ and nonzero with fairly large values for the other UX_2 compounds, which is in agreement with the experimental results. It is concluded that the zero EFG cannot be obtained by using LDA, GGA, regular LDA+U and GGA+U functionals, but it is possible with EECE functional. The origin of the zero EFG for UBi₂ and nonzero for the other compounds is investigated and it is concluded that the antiferromagnetic ordering of $\uparrow\downarrow$ for UBi₂ and more

long-range ordering of $\uparrow\uparrow\downarrow\downarrow$ for UX_2 ($X=Sb, As, P$) are responsible for the difference in the EFG values. The analyses of EFGs show that the magnetic structure and spin arrangement of atoms affect EFG; whereas in the mentioned factors, the magnetic orbitals of uranium have the highest influence on EFGs. Furthermore, valence electrons (Quasi-core) in the MT sphere play an important role in EFG and the contribution of electrons which are out of the MT sphere is very small. The calculated EFG data for different temperatures show that EFG decreases as temperature increases but, this increase in EFG is significant only at high temperatures, whereas at room temperature it is ignorable.

The DOS curves show that uranium atoms are magnetic and X atoms are non-magnetic for all UX_2 compounds. Therefore, in these compounds, magnetic planes of uranium are separated with non-magnetic X planes. So, there is a quasi-two dimensional property in these compounds. As DOS curve of f orbital have non-zero value on Fermi surface, therefore f orbital electrons contribute in conduction. These f orbital electrons are non-localized and show different localization in different compound. We also conclude that uranium 5f electrons are responsible for the large effective mass of the conduction carriers of UX_2 and hence conduction process in these compounds. The f orbital is the magnetic orbital of uranium and its electrons have the highest effect on the magnetization of the atom. Therefore, these f orbital electrons have a significant effect on the EFG of uranium. Furthermore, our calculated magnetic moments for the uranium atom in different compounds are consistent with the experimental results²⁴ as compared to the previously calculated values¹⁷, which are severely underestimated.

V. ACKNOWLEDGMENTS

We are thankful to FarhadJalali-Asadabadi for his very friendly contribution. This work was supported by University of Isfahan (UI), Isfahan, Iran.

REFERENCES

1. S. Jalali Asadabadi, S. Cottenier, H. Akbarzadeh, R. Saki and M. Rots, *Phys. Rev. B*, 2002, **66**, 195103.
2. S. Jalali Asadabadi, *Phys. Rev. B*, 2007, **75**, 205130.
3. P. Blaha, K. Schwarz and P. H. Dederichs, *Phys. Rev. B*, 1988, **37**, 2792.
4. M. Rafiee and S. Jalali Asadabadi, *Comput. Mat. Sci.*, 2009, **47**, 584.
5. E. N. Kaufmann and R. J. Vianden, *Rev. Mod. Phys.*, 1979, **51**, 161.
6. J. Yu, A. J. Freeman, R. Podloucky, P. Herzig and P. Weinberger, *Phys. Rev. B*, 1991, **43**, 532.
7. K. Schwarz, C. Ambrosch-Draxl and P. Blaha, *Phys. Rev. B*, 1990, **42**, 2051.
8. P. Blaha, K. Schwarz and P. Herzig, *Phys. Rev. Lett.*, 1985, **54**, 1192.
9. J. L. Sarrao, L. A. Morales, J. D. Thompson, B. L. Scott, G. R. Stewart, F. Wastin, J. Rebizant, P. Boulet, E. Colineau, G. H. Lander, *Nature*, 2002, **429**, 297.
10. Y. Onuki, Y. Haga, E. Yamamoto, Y. Inada, R. Settia, H. Yamagami and H. Harima, *J. Phys.: Condes. Matter*, 2003, **15**, S1903.
11. Y. Onuki, D. Aoki, P. Wisniewski, H. Shishido, S. Ikeda, Y. Inada, R. Settai, Y. Tokiwa, E. Yamamoto, Y. Haga, T. Maehira, H. Harima, M. Higuchi, A. Hasegawa, and H. Yamagami, *ActaPhysicaPolonica B*, 2001, **32**, 3273.
12. Y. Onuki, R. Settai, H. Shishido, S. Ikeda, T. D. Matsuda, E. Yamamoto, Y. Haga, D. Aoki, H. Harima and H. Yamagami, *J. Opt. Mat.*, 2008, **10**, 1535.
13. G. R. Stewart, *Rev. Mod. Phys.*, 2001, **73**, 797.
14. R. Wawryk, J. Mucha, H. Misiorek and Z. Henkie, *Phil. Mag. Lett.*, 2011, 793.

15. P. G. Pagliuso, N. O. Moreno, N. J. Curro, J. D. Thompson, M. F. Hundley, J. L. Sarrao, Z. Fisk, A.D. Christianson, A.H. Lacerda, B.E. Light and A.L. Cornelius, *Phys. Rev. B*, 2002, **66**, 054433.
16. H. Iwasawa, T. Saitoh, Y. Yamashita, D. Ishii, H. Kato, N. Hamada, Y. Tokura and D. D. Sarma, *Phys. Rev. B*, 2005, **71**, 075106.
17. S. Lebegue, P. M. Oppeneer and O. Eriksson, *Phys. Rev. B* **73**, 045119 (2006).
18. D. Aoki, P. Wisniewski, K. Miyake, N. Watanabe, Y. Inada, R. Settai, E. Yamamoto, Y. Haga and Y. Onuki, *J. Phys. Soc. Jpn.*, 1999, **68**, 2182.
19. D. D. Koelling, B. D. Dunlap and G. W. Crabtree, *Phys. Rev. B*, 1985, **31**, 4966.
20. H.H. Hill, W.N. Miner, *Plutonium and Other Actinides*, The Metallurgical Society of the AIME, New York, 1970.
21. M. Zarshenas, S. Jalali-Asadabadi, *Thin Solid Films*, 2012, **520**, 2901.
22. J. Grunzweig-Genossar, M. Kuznietz and F. Friedman, *Phys. Rev.*, 1968, **173**, 562.
23. R. Troc, and Z. Zolnierrek, *Phys. Phys.*, 1979, **40**, C4-79.
24. G. Amoretti, A. Blaise and J. Mulak, *J. Mag. Mag. Mat.*, 1984, **42**, 65.
25. Fredrik Grønvold, Morad Ramzy Zaki, Edgar F. Westrum Jr., James A. Sommers, and David B. Downie, *J. Inorg. Nucl. Chem.*, 2001, **40**, 635.
26. D. Aoki, P. Winsniewski, K. Miyake, N. Watanabe, Y. Inada, R. Settai, E. Yamamoto, Y. Haga and Y. Onuki, *Phil. Mag. B*, **80**, 1517 (2004).
27. D. Aoki, P. Winsniewski, K. Miyake, R. Settai, Y. Inada, K. Sugiyama, E. Yamamoto, Y. Haga and Y. Onuki, *Physica B*, 2000, **281**, 761.
28. P. Winsniewski, D. Aoki, K. Miyake, N. Watanabe, Y. Inada, R. Settai, Y. Haga, E. Yamamoto and Y. Onuki, *Physica B*, 2000, **281**, 769.

29. P. Winsniewski, D. Aoki, N. Watanabe, K. Miyake, R. Settai, Y. Onuki, Y. Haga, E. Yamamoto and Z. Henkie, *J. Phys. Condens. Matter.*, 2000, **12**, 1971.
30. S. Tsutsui, M. Nakada, S. Nasu, Y. Haga, D. Aoki, P. Wisniewski and Y. Onuki, *Phys. Rev. B*, 2004, **69**, 054404.
31. P. Blaha, K. Schwarz, G. Madsen, D. Kvasnicka and J. Luitz, Vienna Universitat of Technology, Austria (2011).
32. A. H. MacDonald, W. E. Pickett and D. D. Koelling, *J. Phys.*, 1997, **C13**, 2675.
33. P. Hohenberg and W. Sham, *Phys. Rev. B*, 1964, **136**, 864.
34. J. P. Perdew and Y. Wang, *Phys. Rev. B*, 1992, **45**, 13244.
35. J. P. Perdew and A. Zunger, *Phys. Rev. B*, 1981, **23**, 5048.
36. D. M. Ceperley and B. J. Alder, *Phys. Rev. Lett.*, 1980, **45**, 566.
37. J. P. Perdew, K. Burke and M. Ernzerhof, *Phys. Rev. Lett.*, 1996, **77**, 3865.
38. J. P. Perdew, K. Burke and Y. Wang, *Phys. Rev. B.*, 1996, **54**, 16533.
39. D. C. Langreth and J. P. Perdew, *Phys. Rev. B*, 1980, **21**, 5469.
40. Z. Wu and R. E. Cohen, *Phys. Rev. B*, 2006, **73**, 235116.
41. V. I. Anisimov, J. Zaanen and O. K. Andersen, *Phys. Rev. B*, 1991, **44**, 943.
42. V. I. Anisimov, F. Aryasetiawan and A. I. Lichtenstein, *J. Phys.: Cond. Matt.*, 1997, **9**, 767.
43. M. T. Czyzyk and G. A. Sawatzky, *Phys. Rev. B*, 1994, **49**, 14211.
44. V. I. Anisimov, I. V. Solovyev, M. A. Korotin, M. T. Czyzyk and G. A. Sawatzky, *Phys. Rev. B*, 1993, **48**, 16929.
45. F. Tran, F. Karsai and P. Blaha, *Phys. Rev. B*, 2014, **89**, 155106.
46. P. Novak, J. Kunes, L. Chaput and W. E. Pickett, *Phys. Stat. Sol.*, 2006, **243**, 563.

47. A. D. Becke, Phys. Rev. A, 1988, **38**, 3098.
48. E. Guziewicz, T. Durakiewicz, M. T. Butterfield, C. G. Olson, J. J. Joyce, A. J. Arko, J. L. Sarrao, D. P. Moore and L. Morales, Phys. Rev. B, 2004, **69**, 045102.
49. S. Jalali Asadabadi, Ph.D. Thesis, Isfahan University of Technology, 2003.
50. S. K. Mohanta, S. N. Mishra, S. K. Srivastava and M. Rots, Solid. Stat. Comm., 2010, **150**, 1789.
51. S. Cottenier, and M. Rots, "Hyperfine Interactions and their Application in Nuclear Condensed Matter Physics: a microscopic introduction", (Leuven University 2004).